tistical test decides in favor of the null hypothesis: the ether drift velocity is zero.

Another statistical technique that can be used to interpret the results of the ether drift experiment is that of estimation. For instance, what value of the ether drift velocity would be most likely to produce the observed results? This may be calculated by simultaneously maximizing the likelihood ratio, given by Whalen,[8] $\rho = \exp(-A^2N/4\sigma^2)I_0 \times (Aq/\sigma^2)$, with respect to A and σ^2 (I_0 is the zeroth order modified Bessel function of the first kind). This "maximum likelihood" estimate gives an ether drift velocity of 1.5 km/s for the noon observations, and 4.2 km/s for the evening observations. The estimates of σ^2 correspond to velocities of 7.5 km/s for the noon observations and 8.6 km/s for the evening observations. 1.5 and 4.2 km/s are, respectively, about 20 and 7 times smaller than the orbital velocity of the earth. The velocity estimated at noon is smaller than Michelson's and Morley's upper bound by a factor of about four, while the evening estimate is roughly comparable. These values disagree with the 8.8- and 8.0-km/s velocities that Miller claims to have determined from his reanalysis of the 1887 data.[6]

IV. DISCUSSION

The modern approaches discussed above yield the emphatic conclusion: the 1887 observations of Michelson and Morley are not consistent with an ether drift velocity significantly different from zero. This confirms the conclusion drawn by Michelson and Morley, and refutes the one drawn by Miller about their observations. The conclusion drawn by Michelson and Morley has been accepted by most physicists. Miller's conclusions about his own ether drift experiments, namely that there was significant relative motion between the earth and the ether have met with a very different reception. Miller's results were carefully scrutinized by R. S. Shankland *et al.*,[3] who concluded that the apparent either drift velocity was in fact a spurious result of temperature gradients across the interferometer. It is Shankland's appraisal that is most widely accepted. Although the Michelson–Morley experiment has been reviewed,[11,12] neither reviewer mentioned the incompletely detailed data reduction. This is a contrast to the criticism earned by the meticulously described results of Miller, which encourages the speculation that observations supporting a well accepted theory received much less scrutiny than those that do not, regardless of their true individual merits.

ACKNOWLEDGMENTS

I would like to thank Allan Franklin for his enthusiastic encouragement and helpful advice in the completion of this work. I am also grateful to Irving Weiss for his help with the rather involved statistics.

[1]G. Holton, Isis **60**, 133 (1969).
[2]A. A. Michelson and E. W. Morley, Am. J. Sci. **34**, 333 (1887).
[3]R. S. Shankland, S. W. McCuskey, F. C. Leone, and G. Kuerti, Rev. Mod. Phys. **27**, 167 (1955).
[4]F. W. Sears, M. W. Zemansky, and H. D. Young, *University Physics*, 5th ed. (Addison-Wesley, Reading, MA, 1976), p 718.
[5]R. S. Shankland, private communication.
[6]D. C. Miller, Rev. Mod. Phys. **5**, 203 (1933).
[7]A. Ralston and H. Wilf, *Mathematical Methods for Digital Computers* (Wiley, New York, 1960), Chap. 24.
[8]A. D. Whalen, *Detections of Signals in Noise* (Academic, New York, 1971), Chaps. 4 and 7.
[9]M. G. Kendall and A. Stuart, *The Advanced Theory of Statistics* (Griffen, London, 1958), p 461.
[10]M. Abramowitz and I. A. Stegun, *Handbook of Mathematical Functions* (U.S. G.P.O., Washington, DC, 1970), Chap. 26.
[11]R. S. Shankland, Am. J. Phys. **32**, 16 (1964).
[12]L. S. Swenson, J. Hist. Astron. **1**, 56 (1970).

Fourier transforms and the use of a microcomputer in the advanced undergraduate laboratory

D. R. Matthys and F. L. Pedrotti
Marquette University, Milwaukee, Wisconsin 53233

(Received 16 September 1981; accepted for publication 21 January 1982)

An experiment using a standard Michelson interferometer and a microcomputer to produce and display Fourier transform spectrograms in the advanced undergraduate laboratory is described. Fourier transforms of laser and mercury light sources, as well as simulated data from a function generator, are presented and discussed. The computer program used is designed to be highly interactive and to allow the student a wide range of performance options.

INTRODUCTION

Fourier transform spectrometry represents an elegant alternative to traditional methods of spectrum analysis. The special advantages of this technique have led to widespread applications in research and industry. Both its current relevance and the necessary use of a computer in data manipulation make it an attractive experiment for the advanced undergraduate laboratory.

Several papers have appeared[1–5] in this journal elaborating various theoretical and experimental aspects of such an experiment. This paper describes the incorporation of

Fourier transform spectrometry (FTS) into the advanced undergraduate laboratory at Marquette University and is intended to be useful in providing all the essential details for those interested in adding this experiment to their laboratory curriculum. A listing of the computer program developed (in Basic) for interactive execution and display of the results of this experiment will be made available to interested inquirers. After some general discussion of the technique and its application to data generated by a Michelson interferometer, the experimental arrangement and method employed as well as sample results will be presented and discussed. The educational value of this project lies mainly in its coordinated use of three major components: the physics and mathematics of the Fourier transform (FT), the optics of the Michelson interferometer, and the interactive use of a microcomputer in the laboratory.

THEORETICAL

The special advantages of the Fourier transform spectrometer (FTS) derive from the use of a large aperture at signal input and the presence of the entire spectrum at signal output. Thus the FTS is not limited to intensities determined by the narrow slits or wavelength ranges inherent in prism or grating spectrometers. In addition, the FTS technique is capable of high resolution, limited in principle only by the sample width of the input data and the wavelength region being analyzed.

The large aperture and integrated throughput of the Michelson interferometer thus make it useful as an FT spectrometer. It will be shown in the following treatment that the spectral distribution (spectrogram) of the light incident on a Michelson interferometer is just the Fourier transform of the output intensity of its two-beam interference as a function of mirror movement, or the path difference between interfering light beams.

Figure 1 shows schematically the Michelson interferometer, which uses a beam splitter BS to separate equal amplitude portions of a spectral input beam from source S, and reunite them again after reflections from mirrors $M1$ and $M2$. The interfering beams are collected at detector D. The extended source at the input can introduce a small shift in the observed wavelengths and leads to some decrease in resolution. These effects, which are minor for the apparatus used here, are described in detail elsewhere.[6]

Let the electric fields of the interfering beams for a particular wavenumber $k\,(=2\pi/\lambda)$ component in the light source, on arrival at the detector, be represented by

$$E_1 = E_0 \cos(kx_1 - \omega t),$$

$$E_2 = E_0 \cos(kx_2 - \omega t),$$

where the two beams have experienced a path difference of $x = x_2 - x_1$ between separation and recombination. The time-averaged intensity for the k component at the detector is then given by

$$I_k = \langle (E_1 + E_2)^2 \rangle = 2I_0(1 + \cos kx),$$

where I_0 represents the time-averaged intensity of one beam. Since there will be a spread of k values in the source, I_k can be interpreted as intensity $I(k)$ per unit k interval at k, giving an integrated intensity over all wavelengths of

$$I = \int_0^\infty I(k)\, dk = \int_0^\infty 2I_0(k)\, dk + \int_0^\infty 2I_0(k) \cos kx\, dk.$$

The first term in the result represents the constant integrated intensity due to all wavelength components in the two noninterfering beams added together. The second term represents interference between the two beams and can be considered as a positive or negative deviation from the constant term, dependent upon the path difference x. If the first term is considered a mean intensity, then intensity fluctuations about the mean comprise the spectral distribution (interferogram) given by

$$I_m(x) = \int_0^\infty I_m(k) \cos kx\, dk,$$

which is the Fourier transform of the spectrogram,

$$I_m(k) = (2/\pi) \int_0^\infty I_m(x) \cos kx\, dx. \tag{1}$$

Thus measurement of the interferogram output $I_m(x)$ at a point on the optic axis of the system at the detector, as a function of path difference x, allows a calculation of the spectral intensity distribution $I_m(k)$ as a function of wavenumber by the Fourier transform integration indicated in Eq. (1). When the function $I_m(x)$ is a discrete set of sample points, the continuous FT is allowed to go over into sums and is referred to as a discrete Fourier transform (DFT). Because the DFT employs a finite interval (window) of data taken at finite sampling intervals, the following critical consequences must be taken into account, which are more fully discussed elsewhere.[4,6,7]

(a) Restriction of data to a finite window x_w is mathematically equivalent to a multiplication of the continuous function $I_m(x)$ by a rectangular pulse that is nonzero over the width x_w. The FT of this product, which can be shown to be the convolution of the individual FTs, introduces the sinc function which both smears the transform $I_m(k)$ and, if discontinuities are introduced at the boundaries of the sample waveform when the window is periodically extended, introduces "leakage" effects or side bands. These effects of the sinc function, with its large central peak and smaller side lobes, are discussed and exhibited graphically by various authors.[4,7,8] The smearing can be shown to limit the resolution of the spectral distribution so that

$$\Delta(1/\lambda) = 1/x_w$$

or

$$\Delta\lambda = \lambda^2/x_w.$$

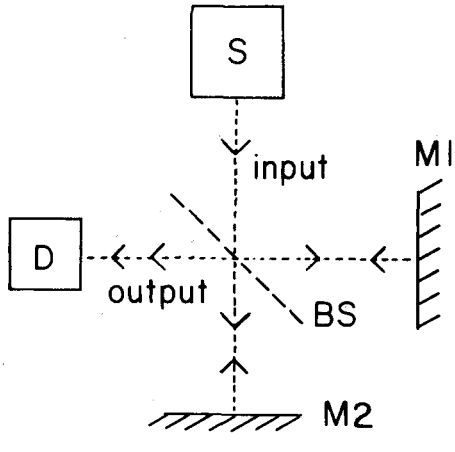

Fig. 1. Basic optics of a Michelson interferometer.

Thus, if the interferometer mirror is translated at such a rate as to accumulate a path difference per second of $x_t = \Delta x/\Delta t$ (nm/s), and the intensity is sampled at a rate $n_t = \Delta n/\Delta t$ (readings/s), the minimum resolvable wavelength interval will be given by

$$(\Delta\lambda)_{\min} = n_t\lambda^2/x_t(N-1), \tag{2}$$

where N is the total number of sampled data points. To achieve optimum resolution for a given N, Eq. (2) indicates that the ratio x_t/n_t (nm/reading) should be as large as possible to produce the largest window. The maximum number of data points is limited by memory storage requirements and by computer time in handling the calculations. The short-wavelength region produces better resolution, but in order to permit visual alignment the experiments suggested here are limited to the visible region of the spectrum. For example, if x_t is 74.5 nm/s and n_t is 2.5 readings/s, a total of 1024 data points gives a $(\Delta\lambda)_{\min}$ of 5.2 nm at 400 nm, and 16.1 nm at 700 nm.

The "leakage" caused by the nonperiodicity of the data sample with the window causes the frequency components involved to spill over into more than one spectral line in the output. Mathematically, this is due to the presence of the lobes of the sinc function; practically, it causes further degradation in the resolution of the spectrogram. A technique called "apodization" (literally, "removal of the feet") can reduce the side bands but with additional loss of resolution. This technique[5-7] multiplies the interferogram by a function (e.g., triangular, trapezoidal, Gaussian, and cosine functions have been used) that reduces the severity of the leakage effect. The consequences of using some of these functions are shown graphically in Ref. (5). For simplicity, our program incorporates the option of using only the triangular function to apodize the data.

(b) The approximation of the true interferogram $I_m(x)$ at a sampling interval $x_s = x_t/n_t$ leads to the phenomenon of "aliasing," such that portions of the spectrogram $I_m(k)$ for wavelengths less than $2x_s$ will be folded back into the spectrum of greater wavelengths, confusing the interpretation. Such overlapping of waveforms can be avoided by observing the Nyquist criterion of sampling theory: the signal must be sampled at a rate at least twice as high as the highest frequency present.[7,9] Interpreted in terms of this experiment, the sampling interval must be less than half the smallest wavelength present in the source in order to avoid aliasing. Expressed in terms of our experimental parameters, the condition is that the minimum wavelength in the source which can be unambiguously handled by the transform calculation is

$$\lambda_{\min} = 2(x_t/n_t). \tag{3}$$

A large ratio of x_t/n_t, while desirable in achieving good resolution, may lead to aliasing by producing too high a value of $\lambda_{\min}$. For example, the values of x_t and n_t given previously require that the source contain no wavelength contributions smaller than about 60 nm. If, however, the rate of taking data was decreased by several times, the short-wavelength end of the visible spectrum could be confused by aliasing.

The number of operations performed by a computer in calculating the spectral distribution $I_m(k)$ is roughly equal to N^2, where N is the number of data points. The Cooley–Tukey algorithm for doing this series of calculations reduces the number of calculations to about $N \log_2 N$, and is known as the "fast Fourier transform" (FFT). Specific details of the FFT algorithm can be found elsewhere.[4,6,7,8] The calculations performed in these experiments employ a version of the FFT.

EXPERIMENTAL METHOD

Figure 2 illustrates schematically the experimental apparatus employed. A broad aperture source of light S to be analyzed admits light to the beam splitter BS after passing through an optional filter F (used when it is desirable to restrict the input bandwidth). If the source is a laser, the beam is first made diverging by a short-focal-length lens such that the light fills both mirrors $M1$ and $M2$. The mirrors may be most easily brought initially into perpendicular alignment by allowing a narrow laser beam to pass through the interferometer and project onto a screen (a white index card is sufficient) positioned in front of the lens L, and by using the adjusting screws on $M2$ to bring the two primary beam spots into coincidence. When properly aligned, a broad aperture light source will produce circular interference fringes at the aperture with the aid of the converging lens L. The center of the pattern is made to fall over the circular aperture, which should not be so large as to accept more than one order of interference. A pinhole diameter of about 1 mm was found to be useful in this work. The micrometer screw of a Beck-Ealing interferometer was fitted with a gear wheel to accept a plastic gear belt providing nonslippage drive when driven by a low speed motor of 2 rpm in tandem with a gear speed reduction of 20:1. The motor and reducer were isolated mechanically from the table supporting the interferometer. Variable diameter gear wheels were useful in providing a variety of rates of mirror movement. The light detector used was a 1P21 photomultiplier tube (S4 spectral response), whose signal was amplified by a Keithley 610 Electrometer. The variety of amplifications available with this electrometer, as well as its 0–3-V output, make it a convenient instrument for simultaneously feeding a strip-chart recorder and providing the interferogram signal to be sampled by the microcomputer.

In practice the chart-recorder trace furnishes a convenient record of the interferogram to be transformed, as well as an immediate indication of bad data. Any mechanical or electrical failure in the system will be registered as an interruption in a smooth recorder trace. The chart recorder is also useful in determining the rate of mirror movement. The linearity of the carriage motion can be checked, and if

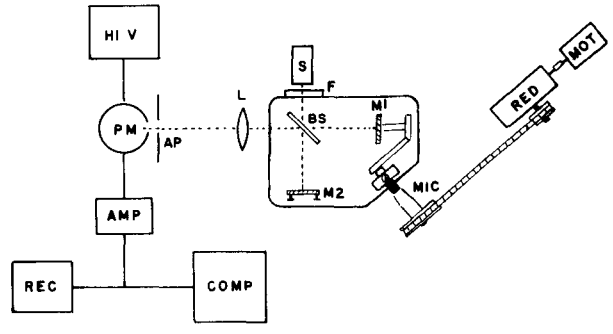

Fig. 2. Schematic of apparatus. Light from a Michelson interferometer with continuous belt drive is detected by a photomultiplier (PM) and recorded by both a strip-chart recorder (REC) and a microcomputer (COMP).

necessary calibrated, using a laser input signal.[10,11] Over the small mirror movements required in these measurements, no significant nonlinearities were experienced. By timing a large number of the interference fringe patterns produced using a helium-neon laser, a reliable value of x_t (nm/s), which is twice the rate of mirror movement, can be determined. The other experimental rate required is n_t, the number of readings taken per second. The program being used allows the computer to read the voltage output of the Keithley electrometer at a selectable rate, which can be accurately determined from the time required to take a large number of readings. For tutorial purposes, the light source and optics can be dispensed with and a simulated signal can be fed to the computer from one or more function generators. Thus the Fourier transform of several sine waves at different frequencies simulating several spectral lines, or of a square pulse or ramp signal, can be analyzed by the same program.

The analysis of the interferogram is done on a microcomputer connected to the 0–3-V output of the Keithley electrometer. Although several programs for doing Fourier transforms are available in the standard journals,[12–14] it quickly becomes apparent that the actual Fourier transform is a very small part of any effective program. The power and value of the program used in our experiment lies in its flexibility and the many choices it offers the student.

The program that performs the Fourier transform on the data is written in North Star Basic and is very interactive, allowing the student a wide range of options: normal or inverse transform, number of samples from 64 to 1024 in steps of powers of 2, sampling rate from milliseconds to seconds, apodization of the data with triangle function, discrete transform (FFT) or an approximation to a continuous transform,[11] CRT graphical display on a 256×256-point grid of either the input voltage data or output spectral data with a hard copy option, a printer listing of results with simple graphics but with values of wavelengths given, and

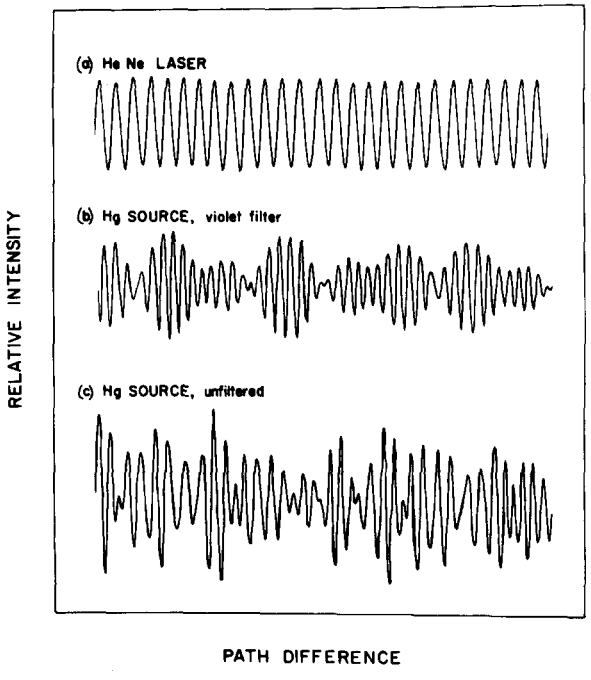

Fig. 3. Strip-chart recorder traces of interferograms due to light from (a) He–Ne laser; (b) Hg source with violet filter; and (c) Hg source, unfiltered.

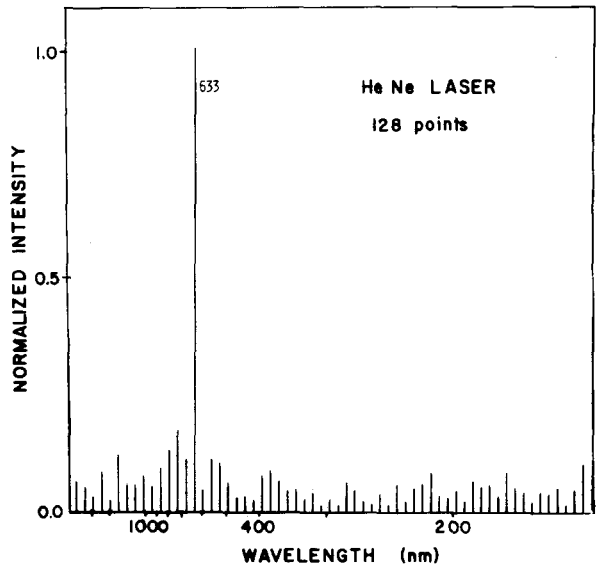

Fig. 4. Spectrogram of light from an He–Ne laser, Fourier transformed from a 128-point interferogram.

the ability to save the data on a magnetic disk. The program requires about 12K of memory, not including space for data arrays. The additional data storage requirements can be quite extensive if it is desired to do 1024 sample points.

Although one of the main purposes of the experiment is to familiarize the student with the use of a microcomputer in the laboratory, the student is not expected to do any programming. An introductory lecture is given explaining the Fourier transform and the significance of the various parameters involved; later, when the student actually performs the experiment, the program asks what value the student wishes to assign to each parameter. On the other hand, many of the students have some familiarity with the Basic language and are able to examine the program to see how it works.

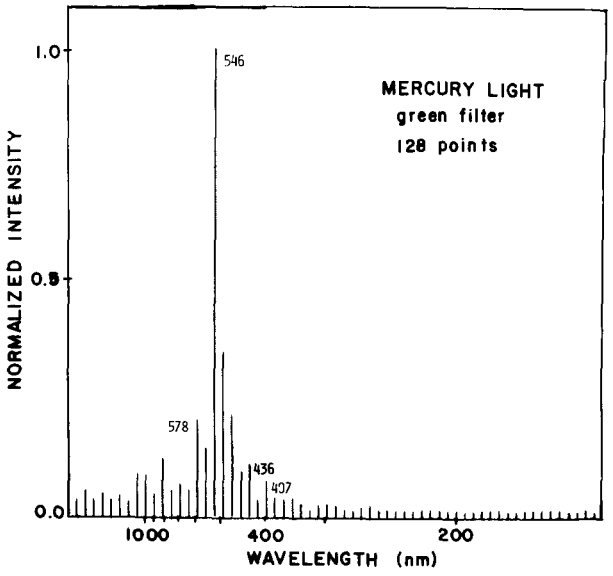

Fig. 5. Spectrogram of mercury light filtered by a broad-band green filter, Fourier transformed from a 128-point interferogram.

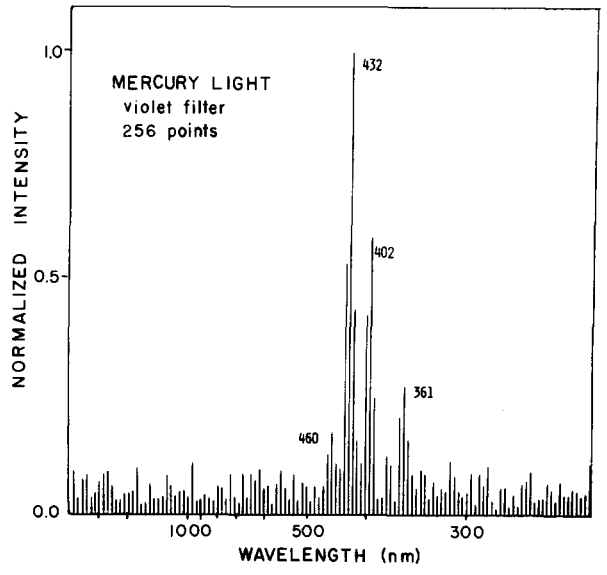

Fig. 6. Spectrogram of mercury light filtered by a broad-band violet filter, Fourier transformed from a 256-point interferogram.

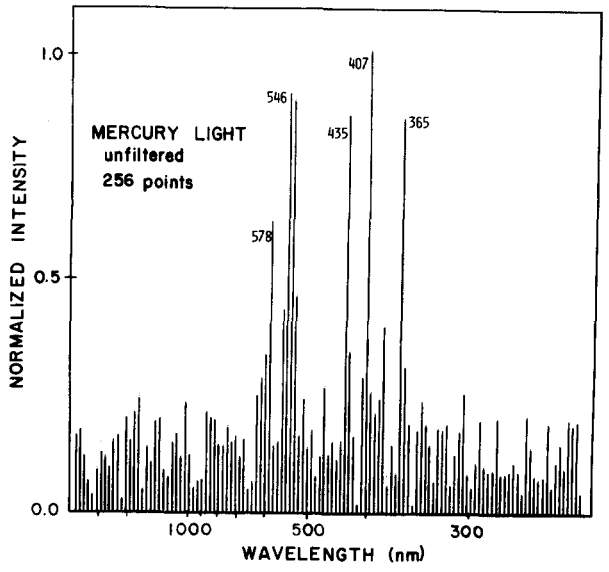

Fig. 7. Spectrogram of mercury light, filtered only by glass optics, Fourier transformed from a 256-point interferogram.

Because the program is written in Basic it runs rather slowly; an FFT of 256 points takes about two and a half minutes. The microcomputer system used is a North Star system with 56K memory and two disk drives connected to a standard CRT terminal and a small printer. Two specialized items are also used, a slow speed 12-bit analog-to-digital converter[15] to prepare the Keithley output voltage signal for digital processing by the North Star, and a 256×256-pixel graphics board[16] driving a CRT monitor.

RESULTS AND DISCUSSION

Samples of interferograms and spectrograms are shown in Figs. 3–8. In Fig. 3, the interferograms recorded by a strip chart recorder are shown for a monochromatic source using a low-power helium-neon laser, and a mercury discharge lamp source, with and without a filter that transmits predominantly the two strong mercury emissions at 436 (blue) and 405 (violet) nm. The interferogram (b) shows the distinctive beat interference pattern for a two-frequency source. The interferogram (c) for the unfiltered Hg source, including all the mercury emissions longer than 360 nm, illustrates a more complicated interference pattern.

The data from such interferograms is Fourier transformed by the computer to produce spectrograms such as those shown in Figs. 4–8. In each case the wavelength scale divisions are the same as the minimum resolvable $\Delta\lambda$ at λ; hence divisions are not regular. The spectrogram of Fig. 4 results from the helium-neon laser source at 632.8 nm. Effects of finite window, leakage, and noise are clearly evident. Spectrograms of Figs. 5 and 6 correspond to mercury sources using green and violet filters, respectively. The green-filtered Hg light is dominated by the 546-nm Hg emission, although some transmission of the yellow and violet are noticeable. The precision with which the peaks can be located in each case is limited by the resolution, as determined by Eq. (2). The spectrogram of Fig. 7 displays the result of a Fourier transform for unfiltered Hg light, where the major Hg line emissions can be identified, as shown. Pertinent experimental parameters for each spectrogram are given in Table I.

Figure 8 shows several spectrograms that result from simulated data provided by a wave function generator. In this case, the minimum resolvable frequency, which is the frequency scale increment, is more easily determined as the reciprocal of the time window of the measurements. The data for all the spectrograms in Fig. 5 consist of 128 points, taken over a period of 2 s using a frequency of 2 Hz. Spectrogram (a) results from the input of a single sine wave simulating a monochromatic source. Spectrograms (b) and (c) are of triangular and square wave inputs, respectively,

Table I. Values of experimental parameters applicable to the spectrograms of Figs. 4–7. Here N is the total number of data points; n_t is the rate at which spectrogram data is sampled; x_t is twice the rate of mirror movement; $(\Delta\lambda)_{min}$ is the minimum resolvable wavelength interval; and λ_{min} is the minimum wavelength which can be analyzed without aliasing.

Spectrogram	N	n_t (rdg/s)	x_t (nm/s)	$(\Delta\lambda)_{min}$ nm (at 400 nm)	λ_{min} (nm)
(a) He–Ne laser	128	2.03	143	17.9	141
(b) Hg, violet filter	256	1.28	143	5.6	224
(c) Hg, green filter	128	2.03	143	17.9	141
(d) Hg, unfiltered	256	1.28	143	5.6	224

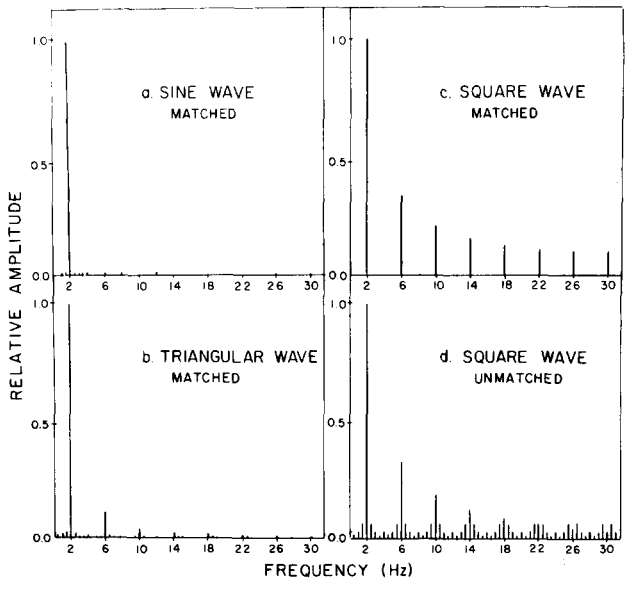

Fig. 8. Fourier-transformed spectrograms of simulated data from a function generator. The sampled data is of (a) sine wave, (b) triangular wave, (c) and (d) square wave. All of the functions have a frequency of 2 Hz. Spectrograms (c) and (d) illustrate the importance of matching the function to the sampling window.

and display the odd harmonics of the Fourier analysis in decreasing amplitude with frequency. The sequence of amplitudes agree with the expected ratios 1:1/3:1/5:1/7... for the square wave and 1:1/9:1/25:1/49... for the triangular wave. The spectrogram given in Fig. 5(c) shows the DFT of a square wave (unapodized) which "matches" the data window (if the wavelength of the fundamental matches the data window, so will the wavelengths of all the higher harmonics); for comparison, Fig. 5(d) shows the spectrogram of an "unmatched" square wave. Since the calculations assume a periodic function, this situation, described earlier as the "leakage" effect, introduces a periodic function at variance with the simple square wave used.

CONCLUSIONS

A wide variety of examples of Fourier transforms can be made available to the optics or advanced laboratory student using a Michelson interferometer as a Fourier spectrometer, coupled with a microcomputer of modest capability. This system can handle real data in the form of output from a Michelson interferometer as well as simulated data generated by one or more standard function generators. In addition, computer-generated functions can also be Fourier analyzed. Since a graphics capability is available to the system, both interferograms and spectrograms can be visually displayed. The experiment is meant only to teach the physics of the technique; it cannot produce the high resolution so attractive in commercial instruments. Standard Michelson interferometers in the instructional laboratory lack the precision of mirror translation that allows large path differences that are sufficiently smooth and maintain proper mirror alignment. Furthermore, the limited memory available in a microcomputer restricts the total number of data points that can be Fourier analyzed. Both of these limitations prevent improved resolutions. Nevertheless, results with this system are impressive and have been successful in introducing students to a powerful technique for spectral analysis with wide-ranging current applications.

ACKNOWLEDGMENT

The authors wish to thank Thaddeus Burch for helpful discussions and technical assistance in the pursuit of this work.

[1]D. K. Berkey and A. L. King, Am. J. Phys. **40**, 267 (1972).
[2]J. C. Albergotti, Am. J. Phys. **40**, 1070 (1972).
[3]J. H. Blatt, D. S. Porterfield, and D. J. Ulmer, Am. J. Phys. **41**, 116 (1973).
[4]R. J. Higgins, Am. J. Phys. **44**, 766 (1976).
[5]J. E. Harvey, Am. J. Phys. **49**, 747 (1981).
[6]Robert John Bell, *Introductory Fourier Transform Spectroscopy* (Academic, New York, 1972).
[7]E. Oran Brigham, *The Fast Fourier Transform* (Prentice-Hall, Englewood Cliffs, NJ, 1974).
[8]G. D. Bergland, IEEE Spectr. **6**, (7), 41 (1969).
[9]It is interesting to note that this criterion is also used in the production of modern digital audio recordings, where an audio signal sampling rate of 50 kHz ensures accurate reproduction of the maximum audio frequency of 20 kHz.
[10]L. J. Gagliardi, Am. J. Phys. **42**, 249 (1974).
[11]R. G. Layton and J. K. Brower, Am. J. Phys. **43**, 180 (1975).
[12]P. K. Bice, Electron. Design **18** (9), 66 (1970).
[13]F. R. Ruckdeshel, Byte **4** (12), 10 (1979). See also the discussion in Byte **5** (4), 12 (1980).
[14]W. D. Stanley and S. J. Peterson, Byte **3** (12), 14 (1978).
[15]Vector Graphic, Inc., 31364 Viak Colinas, Westlake Village, CA 91361. Precision Analog Interface Board. An alternate, but more elaborate, implementation of the interface between the analog signal and the microcomputer digital input is given by D. Cosgrove in Byte **6** (11), 84 (1981).
[16]Matrox Electronic Systems, Inc., 5800 Andover Ave., T. M. R., Quebec, H4T 1H4, Canada. ALT-512 Graphics Display for the S-100 Bus.